

Eguchi, Kei; Shibata, Akira; Kuwahara, Kyoka; Ishibashi, Takaaki

Article

Design of an inductor-less step-up ac/dc converter for 0.3 V 1 MHz vibration energy harvesting

Energy Reports

Provided in Cooperation with:

Elsevier

Suggested Citation: Eguchi, Kei; Shibata, Akira; Kuwahara, Kyoka; Ishibashi, Takaaki (2020) : Design of an inductor-less step-up ac/dc converter for 0.3 V 1 MHz vibration energy harvesting, Energy Reports, ISSN 2352-4847, Elsevier, Amsterdam, Vol. 6, Iss. 2, pp. 159-165, <https://doi.org/10.1016/j.egyr.2019.11.057>

This Version is available at:

<https://hdl.handle.net/10419/243873>

Standard-Nutzungsbedingungen:

Die Dokumente auf EconStor dürfen zu eigenen wissenschaftlichen Zwecken und zum Privatgebrauch gespeichert und kopiert werden.

Sie dürfen die Dokumente nicht für öffentliche oder kommerzielle Zwecke vervielfältigen, öffentlich ausstellen, öffentlich zugänglich machen, vertreiben oder anderweitig nutzen.

Sofern die Verfasser die Dokumente unter Open-Content-Lizenzen (insbesondere CC-Lizenzen) zur Verfügung gestellt haben sollten, gelten abweichend von diesen Nutzungsbedingungen die in der dort genannten Lizenz gewährten Nutzungsrechte.

Terms of use:

Documents in EconStor may be saved and copied for your personal and scholarly purposes.

You are not to copy documents for public or commercial purposes, to exhibit the documents publicly, to make them publicly available on the internet, or to distribute or otherwise use the documents in public.

If the documents have been made available under an Open Content Licence (especially Creative Commons Licences), you may exercise further usage rights as specified in the indicated licence.



<https://creativecommons.org/licenses/by-nc-nd/4.0/>

The 6th International Conference on Power and Energy Systems Engineering (CPESE 2019),
September 20–23, 2019, Okinawa, Japan

Design of an inductor-less step-up ac/dc converter for 0.3 V@1 MHz vibration energy harvesting

Kei Eguchi^{a,*}, Akira Shibata^a, Kyoka Kuwahara^a, Takaaki Ishibashi^b

^a Department of Information Electronics, Fukuoka Institute of Technology, 3-30-1 Wajirohigashi, Higashi-ku, Fukuoka, 811-0295, Japan

^b Department of Electronics Engineering and Computer Science, National Institute of Technology, Kumamoto College, 2659-2 Suya, Koushi-shi, Kumamoto, 861-1102, Japan

Received 2 October 2019; accepted 22 November 2019

Abstract

For vibration energy harvesting, we propose an inductor-less step-up ac/dc converter in this paper. To realize the inductor-less design, the proposed ac/dc converter consists of two converter blocks: Cockcroft–Walton circuit and charge pump. Unlike existing ac/dc converters for vibration energy harvesting, the proposed ac/dc converter can achieve less electro-magnetic interference (EMI), because no magnetic component is necessary. Furthermore, owing to the Cockcroft–Walton circuit, a full-bridge circuit is not necessary to convert vibration energy. Therefore, small vibration energy, namely, as 0.3 V@1 MHz, can be converted directly to dc voltage. Through theoretical analysis and simulation program with integrated circuit emphasis (SPICE) simulation, the performance of the proposed converter with 6× voltage gain is investigated, where the proposed converter is designed by assuming 0.18 μm CMOS process. The proposed converter demonstrates that about 62% power efficiency can be provided, where the output power is 30 μW, the output voltage is about 1.6 V, and the ripple factor is 0.8%. Furthermore, the feasibility of the proposed ac/dc converter is confirmed by breadboard experiments. The inductor-less design provides us to integrate the proposed ac/dc converter into a hybrid IC chip.

© 2019 Published by Elsevier Ltd. This is an open access article under the CC BY-NC-ND license (<http://creativecommons.org/licenses/by-nc-nd/4.0/>).

Peer-review under responsibility of the scientific committee of the 6th International Conference on Power and Energy Systems Engineering (CPESE 2019).

Keywords: Vibration energy harvesting; ac/dc converters; Inductor-less converters; Cockcroft–Walton circuit; Charge pump; CMOS circuits

1. Introduction

Over the past few decades, wireless sensor network (WSN) systems [1] are receiving much attention for monitoring various environment parameters. The bottleneck of the WSN systems is the limited lifetime of WSN nodes, because the WSN nodes are usually driven by a battery source. For this reason, in order to extend lifetime of WSN nodes, some of wasted energy are captured by energy harvesting collectors and are used as a power supply source in recent years.

* Corresponding author.

E-mail address: eguti@fit.ac.jp (K. Eguchi).

<https://doi.org/10.1016/j.egy.2019.11.057>

2352-4847/© 2019 Published by Elsevier Ltd. This is an open access article under the CC BY-NC-ND license (<http://creativecommons.org/licenses/by-nc-nd/4.0/>).

Peer-review under responsibility of the scientific committee of the 6th International Conference on Power and Energy Systems Engineering (CPESE 2019).

There are several types of ambient energy sources, such as solar, wind, vibration, thermoelectric. Among others, we focused on vibration energy, which is a kind of kinetic energy, because it widely exists in the ambient, including the vibration of industrial machinery, transportation vibration, body movement, and so on. In the energy harvesting collectors, the ambient energy is converted into electrical energy by power converters. To utilize vibration energy, an ac/dc converter is necessary as a vital component of energy harvesting collectors. For this reason, several types of ac/dc converters have been proposed in recent years. For example, Shi et al. [2] suggested the ac/dc converter by combining a full-bridge circuit with two buck-boost converters. Wang et al. [3] designed the ac/dc converter by combining a full-bridge circuit with a synchronized switching harvesting on inductor. Shareef et al. [4] realized the ac/dc converter without full-bridge circuits. However, due to the magnetic component, such as inductors, these existing converters becomes bulky. Furthermore, these converters are applied only for low frequency ac input. To solve these problems, we undertake the development of an inductor-less ac/dc converter for vibration energy harvesting.

In this paper, an inductor-less step-up ac/dc converter is proposed for vibration energy harvesting. Unlike existing ac/dc converters for vibration energy harvesting, the inductor-less design of the proposed ac/dc converter is achieved by combining two converter blocks: Cockcroft–Walton circuit [5] and charge pump [6–8]. Owing to the inductor-less topology, small EMI can be provided by the proposed ac/dc converter. Furthermore, the proposed converter can convert AC 0.3 V@1 MHz into a stepped-up DC voltage directly without full-bridge circuit. To clarify the characteristics of the proposed converter with $6\times$ voltage gain, theoretical analysis, SPICE simulations, experiments, and performance comparisons are conducted between the proposed ac/dc converter and existing ac/dc converters [2–4] for vibration energy harvesting.

2. Circuit configuration

The circuit configuration of the proposed ac–dc converter is shown in Fig. 1, where we assume that the input V_{in} ($= 0.3 \text{ V}@1 \text{ MHz}$) is obtained by vibration energy harvesting. As Fig. 1 shows, the proposed converter consists of two converter blocks: First converter block and Second converter block, where the first converter block is called the Cockcroft–Walton circuit [5] and the second converter block is called the charge pump circuit [6–8]. Unlike existing ac/dc converters, the proposed converter has no full-bridge circuit by cascading the Cockcroft–Walton circuit and a charge pump circuit, where the charge pump circuit can be integrated into an IC chip by using CMOS technologies. By driving switches S_1 and S_2 by two-phase clock pulses, the proposed ac/dc converter generates the output voltage:

$$V_{out} = 2 \times 3 \times V_{in} = 6 \times V_{in} \quad (1)$$

because the voltage gain of the first converter is $2\times$ and the voltage gain of the first converter is $3\times$. Of course, the voltage gain is proportion to the number of stages. Therefore, the voltage gain can be increased by the number of stages.

3. Theoretical analysis

In this section, theoretical analysis is conducted by using the four-terminal equivalent model [9] shown in Fig. 2. In Fig. 2, m is the turn ratio of an ideal transformer, R_{SC} is the internal resistance of the power converter, and R_L is the output load. To simplify the theoretical analysis, we assume that 1. Parasitic elements are small, 2. Time constant is much larger than the period of clock pulses, and 3. V_{in} is a square wave. The equivalent circuit of the proposed ac/dc converter is derived by combining the equivalent circuits of the first converter block and the second converter block.

In the first converter block, the instantaneous equivalent circuit is expressed as Fig. 3, where R_d is the on-resistance of the diode, V_{th} is the threshold voltage, $\Delta q_{T_i, v_{in}}$ ($i = 1, 2$) is the electric charge of V_{in} in State- T_i , and $\Delta q_{T_i, v_o}$ is the electric charge of the output terminal in State- T_i . In a steady state, the differential value $\Delta q_{T_i}^k$ of the capacitors, C_1 , C_2 , and C_3 , satisfy

$$\Delta q_{T_1}^k + \Delta q_{T_2}^k = 0, \quad \text{where } T = T_1 + T_2 \text{ and } T_1 = T_2 = T/2 \quad (2)$$

Because the electric charges of C_k are the same at the start and end of the cycle T . Using Eq. (2), we obtain the following equations by using Kirchhoff's current law:

$$\Delta q_{T_1, v_{in}} = -\Delta q_{T_1}^2 - \Delta q_{T_1}^3, \quad \Delta q_{T_1, v_o} = \Delta q_{T_1}^1 + \Delta q_{T_1}^2 + \Delta q_{T_1}^3 \quad (3)$$

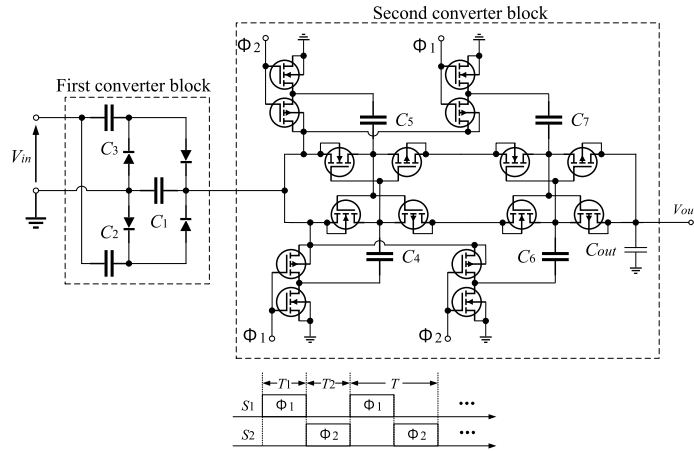


Fig. 1. Circuit configuration of the proposed dual-input cross-connected charge pump with 6× step-up gain.

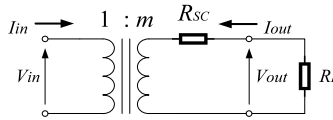


Fig. 2. Four-terminal equivalent model.

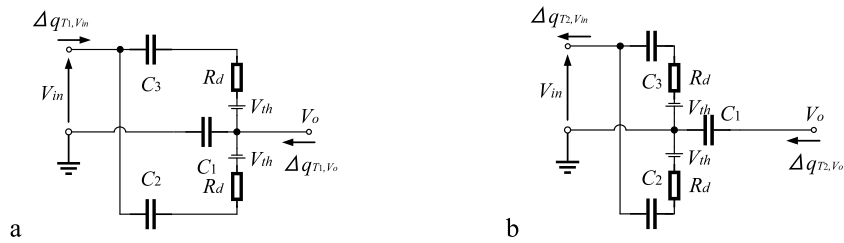


Fig. 3. Instantaneous equivalent circuits of the first converter block: (a) state- T_1 ; (b) state- T_2 .

$$\Delta q_{T_2, v_{in}} = \Delta q_{T_2}^2 + \Delta q_{T_2}^3, \quad \Delta q_{T_2, v_o} = \Delta q_{T_2}^1 \tag{4}$$

$$\Delta q_{T_1}^2 = \Delta q_{T_1}^3, \quad \text{and} \quad \Delta q_{T_2}^2 = \Delta q_{T_2}^3 \tag{5}$$

From Eqs. (2)–(5), the average input/output currents, I_{in} and I_o , are expressed as

$$I_{in} = \frac{\Delta q_{v_{in}}}{T} = \frac{\Delta q_{T_1, v_{in}} + \Delta q_{T_2, v_{in}}}{T} \quad \text{and} \quad I_o = \frac{\Delta q_{v_o}}{T} = \frac{\Delta q_{T_1, v_o} + \Delta q_{T_2, v_o}}{T} \tag{6}$$

Because the overall change in the electric charges, $\Delta q_{T_i, v_{in}}$ and $\Delta q_{T_i, v_o}$, is zero in the steady state. Therefore, we have the following relation between the input and the output by substituting Eqs. (2)–(5) into Eq. (6):

$$I_{in} = -2I_o \text{ and } \Delta q_{v_{in}} = -2\Delta q_{v_o} \tag{7}$$

Therefore, the parameter m_1 is 2.

Next, we discuss the total consumed energy, W_T , of Fig. 3 in order to derive R_{SC} . From Fig. 3, W_T is expressed as

$$W_T = W_{T1} + W_{T2} = 2R_d \frac{(\Delta q_{v_o})^2}{T}, \tag{8}$$

Because the consumed energy in State- T_1 and State- T_2 is given by

$$W_{T1} = R_d \frac{(\Delta q_{T1}^2)^2}{T_1} + R_d \frac{(\Delta q_{T1}^3)^2}{T_1} = R_d \frac{(\Delta q_{v_o})^2}{T} \quad \text{and} \quad W_{T2} = R_d \frac{(\Delta q_{T2}^2)^2}{T_2} + R_d \frac{(\Delta q_{T2}^3)^2}{T_2} = R_d \frac{(\Delta q_{v_o})^2}{T}. \quad (9)$$

From Eqs. (8) and (9), we get the internal resistance of the first converter block, R_{SC1} , as $2R_d$, because W_T of Fig. 3 can be expressed as

$$W_T \triangleq \left(\frac{q_{v_{out}}}{T} \right)^2 R_{SC} T \quad (10)$$

Next, the instantaneous equivalent circuit of the second converter block is expressed as Fig. 4, where R_{Non} is the on-resistance of the NMOS transistor, R_{Pon} is the on-resistance of the PMOS transistor, $\Delta q_{T_i, v_i}$ ($i = 1, 2$) is the electric charge of V_i in State- T_i , and $\Delta q_{T_i, v_{out}}$ is the electric charge of the output terminal in State- T_i . In Fig. 4, the differential value $\Delta q_{T_i}^k$ of the capacitors, C_4, \dots, C_7 , and C_{out} , also satisfy Eq. (2) in a steady state. Using Eq. (2), we have

$$\Delta q_{T1, v_i} = \Delta q_{T1}^4 - \Delta q_{T1}^5 - \Delta q_{T1}^6, \quad \Delta q_{T1, v_{out}} = \Delta q_{T1}^6 + \Delta q_{T1}^{out}, \quad (11)$$

$$\Delta q_{T2, v_i} = -\Delta q_{T2}^4 + \Delta q_{T2}^5 - \Delta q_{T2}^7, \quad \Delta q_{T2, v_{out}} = \Delta q_{T2}^7 + \Delta q_{T2}^{out}, \quad (12)$$

$$\Delta q_{T1}^5 = -\Delta q_{T1}^7, \quad \Delta q_{T2}^4 = -\Delta q_{T2}^6, \quad \text{and} \quad \Delta q_{T1}^5 = \Delta q_{T2}^4, \quad (13)$$

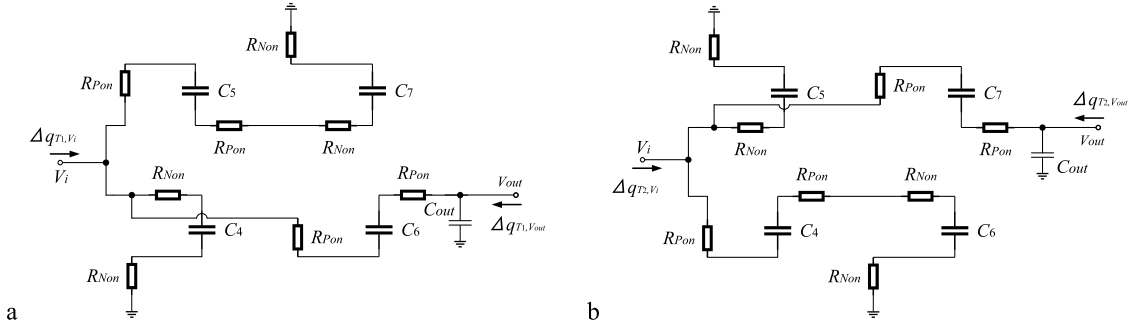


Fig. 4. Instantaneous equivalent circuits of the second converter block: (a) state- T_1 ; (b) state- T_2 .

From Eqs. (2), (6), and (11)–(13), the average input/output currents, I_i and I_{out} , can be obtained as

$$I_i = -3I_{out} \quad \text{and} \quad \Delta q_{v_i} = -3\Delta q_{v_{out}} \quad (14)$$

Therefore, the parameter m_2 is 3.

On the other hand, the total consumed energy of the second converter block is given by

$$W_T = W_{T1} + W_{T2} = 2W_{T1}, \quad (15)$$

Because

$$W_{T1} = 2R_{Non} \frac{(\Delta q_{T1}^4)^2}{T_1} + 2R_{Pon} \frac{(\Delta q_{T1}^6)^2}{T_1} + 2(R_{Non} + R_{Pon}) \frac{(\Delta q_{T1}^5)^2}{T_1}, \quad (16)$$

Since Eqs. (15) and (16) can be rewritten as

$$W_T = 4(R_{Non} + R_{Pon}) \frac{(\Delta q_{v_{out}})^2}{T}, \quad (17)$$

We have the internal resistance of the second converter block, R_{SC2} , as $4(R_{Non} + R_{Pon})$ from Eq. (10). Finally, by using m_1 , R_{SC1} , m_2 , and R_{SC2} , the equivalent circuit of the proposed converter can be derived as shown in Fig. 5. From Fig. 5, we can estimate the maximum output voltage and the maximum power efficiency as

$$V_{out} = 6V_{in} \times \left\{ \frac{R_L}{R_L + 9R_{SC1} + R_{SC2}} \right\} \quad \text{and} \quad \eta = \frac{R_L}{R_L + 9R_{SC1} + R_{SC2}} \quad (18)$$

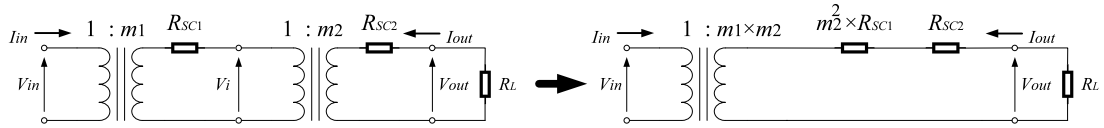


Fig. 5. Equivalent circuit of the proposed converter.

4. SPICE simulation

To clarify the characteristics of the proposed converter, the proposed ac/dc converter was designed by assuming 0.18 μm CMOS process. SPICE simulations were conducted concerning Fig. 1, where the parameters were set to $V_{in} = 0.3 \text{ V@1 MHz}$, $R_{on} = 1 \Omega$, $T_1 = T_2 = 1 \text{ MHz}$, $C_1 = \dots = C_3 = 10 \text{ nF}$, and $C_4 = \dots = C_7 = 100 \text{ pF}$, and $C_{out} = 200 \text{ pF}$. Although the IC integration of the first converter block is impossible due to the capacitor size, the second converter block can integrate into an IC chip.

First, Fig. 6 shows the simulated output voltage as a function of time when $R_L = 100 \text{ k}\Omega$. As you can see from Fig. 6, the proposed converter can offer more than 1.5 V by converting a small input $V_{in} = 0.3 \text{ V@1 MHz}$. Next, in Fig. 7, the power efficiency of the proposed converter is demonstrated as a function of output power. The proposed converter can achieve about 62% power efficiency when the output power is 30 μW . Then, the simulated ripple factor is depicted in Fig. 8. When the output power is 30 μW , the ripple factor is about 0.8%. Finally, Table 1 shows the comparison of characteristics between the proposed ac/dc converter and existing state-of-the-art ac/dc converters [2–4]. Unlike existing converters, the proposed converter can achieve small EMI, because no magnetic component is necessary. Furthermore, the proposed converter can provide the stepped-up voltage by converting the small input voltage, namely, 0.3 V@1 MHz, because the Cockcroft–Walton circuit is employed instead of a full-bridge circuit. Since the input voltage of the proposed converter is smaller than that of the existing converters, the power efficiency of the proposed converter is lower than that of the existing converters. Because the voltage drops caused by diode switches become high in proportion to the decrease of the input voltage.

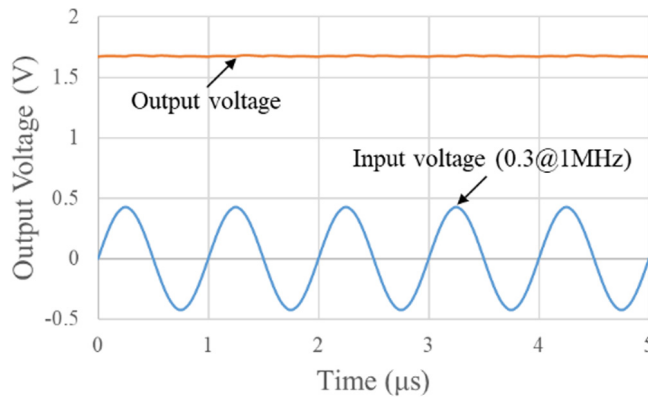


Fig. 6. Simulated output voltage as a function of time.

5. Experiments

To validate the feasibility of the proposed ac/dc converter, the experiment was conducted concerning the experimental circuit which was synthesized with commercially available ICs, namely, Schottky diodes 11EQS03L, photo MOS relays AQV 212, darlington sink drivers TD62004APG, a microcontroller PIC, and electrolytic capacitors, on a breadboard. Fig. 9 demonstrates the measured output voltage when $R_L = 100 \text{ k}\Omega$. As Fig. 9 shows, the experimental circuit can convert AC 0.3 V@1 MHz into DC 1.47 V. The measured output of Fig. 9 is close to the simulated result of Fig. 6. Therefore, we can confirm the feasibility of the proposed ac/dc converter by Figs. 6 and 9.

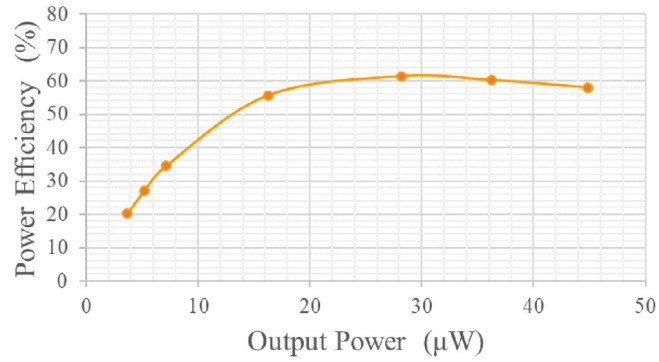


Fig. 7. Simulated power efficiency as a function of output power.

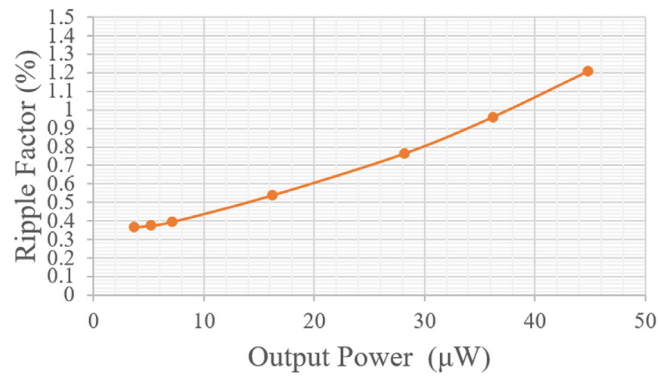


Fig. 8. Simulated ripple factor as a function of output power.

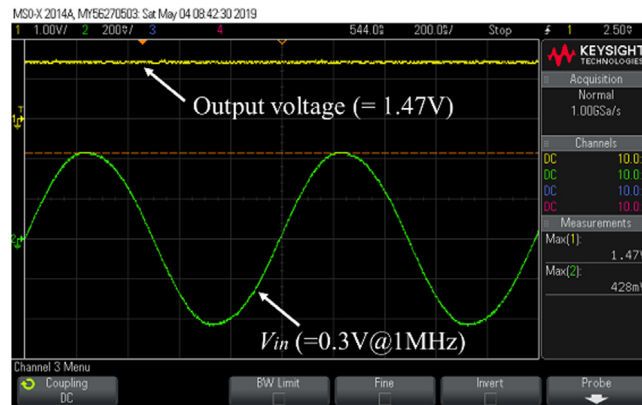


Fig. 9. Measured output voltage.

6. Conclusion

In this paper, an inductor-less step-up ac/dc converter has been proposed for vibration energy harvesting. The performance evaluation and characteristic comparison revealed that 1. The proposed converter can achieve less EMI, because no magnetic component is necessary; 2. Without full-bridge circuits, the proposed converter can offer the 6× stepped-up voltage from small vibration energy; 3. When the output power is 30 μW, the proposed converter can achieve about 62% power efficiency; and 4. The feasibility was confirmed by breadboard experiments, where the experimental circuit converted AC 0.3 V@1 MHz into DC 1.47 V.

Table 1. Comparison of characteristics between the proposed ac/dc converter and existing ac/dc converters.

Topology	Topology	Magnetic component	Input voltage	Frequency of input voltage	Power efficiency
Proposed converter	Cockcroft–Walton + charge pump	Not necessary	0.3 V ~	1 MHz	62% (Input: 0.3 V)
Shi et al. [2]	Full-bridge circuit + bidirectional buck-boost converter + buck-boost converter	Necessary	3.54–25 V	50 Hz	80.6% (Input: 25 V)
Wang et al. [3]	Full-bridge circuit + synchronized switching harvesting on inductor	Necessary	N/A	13.5 Hz	N/A
Shareef et al. [4]	Bidirectional switching converter	Necessary	Up to 3.5 V	N/A	80% (Input: 5 V)

References

- [1] Jayavignesh Thyagarajan, Sundararajan Subashini. A quasi-mobile sink model to optimize deployment, energy and routing cost for scalable static IoT based wireless sensor network. *Int J Intell Eng Syst* 2019;121:263–76.
- [2] Shi Ge, Xia Yinshui, Xia Huakang, Wang Xiudeng, Qian Libo, Chen Zhidong, et al. An efficient power management circuit based on quasi maximum power point tracking with bidirectional intermittent adjustment for vibration energy harvesting. 2019, *IEEE Early Access Articles*.
- [3] Wang Hong-bin, Pan Cheng-liang, Yu Wang, Xia Hao-jie, Yu Lian-Dong. Comparison of interface circuits for piezoelectric wind energy harvesting from galloping oscillation. In: *Proc. of 2019 symposium on piezoelectricity, acoustic waves and device applications*; 2019. p. 1–5.
- [4] Shareef Arish, Ling G Wang, Narasimalu Srikanth, Gao Yuan. A Rectifier-less AC–DC interface circuit for ambient energy harvesting from low-voltage piezoelectric transducer array. *IEEE Trans Power Electron* 2019;342:1446–57.
- [5] Eguchi Kei, Wongjan Anan, Julsereewong Amphawan, Do Wanglok, Oota Ichirou. Design of a high-voltage multiplier combined with Cockcroft–Walton voltage multipliers and switched-capacitor AC-AC converters. *Int J Innovative Comput Inf Control* 2017;133:1007–19.
- [6] Eguchi Kei, Fujimoto Kuniaki, Sasaki Hirofumi. A hybrid input charge-pump using micropower thermoelectric generators. *IEEJ Trans Electr Electron Eng* 2012;74:415–22.
- [7] Abe Kanji, Smerpitak Krit, Pongswatd Sawai, Oota Ichirou, Eguchi Kei. A step-down switched-capacitor AC-DC converter with double conversion topology. *Int J Innovative Comput Inf Control* 2017;131:319–30.
- [8] Wang Yu, Yan Na, Min Hao, Richard Shi C-J. A high-efficiency split-merge charge pump for solar energy harvesting. *IEEE Trans Circuits Syst II* 2017;645:545–9.
- [9] Eguchi Kei, Do Wanglok, Kittipanyangam Soranut, Abe Kanji, Oota Ichirou. Design of a three-phase switched-capacitor ac-ac converter with symmetrical topology. *Int J Innovative Comput Inf Control* 2016;125:1411–21.